Proteins involved in the endoplasmic reticulum stress are key players in synovitis of osteoarthritis, chronic pyrophosphate arthropathy and rheumatoid arthritis, and correlate with the histological score

Dominique de Seny (ddeseny@chuliege.be)
Laboratory of rheumatology, GIGA Research, CHU Liège
Elettra Bianchi
CHU de Liege - Hopital du Sart Tilman
Dominique Baiwir
Universite de Liege
Gaël Cobraiville
Centre hospitalier universitaire de Liege
Charlotte Collin
Universite de Liege
Mégane Deliège
Universite de Liege
Marie-Joëlle Kaiser
Centre hospitalier universitaire de Liege
Gabriel Mazzucchelli
Universite de Liege
Jean-Philippe Hauzeur
Centre hospitalier universitaire de Liege
Philippe Delvenne
Centre hospitalier universitaire de Liege
Michel Malaise
Centre hospitalier universitaire de Liege

Research article

Keywords: proteomic, synovitis, endoplasmic reticulum, biomarker, chaperone, S100A8, S100A9, complement

Posted Date: March 24th, 2020

DOI: https://doi.org/10.21203/rs.3.rs-18867/v1

Proteins involved in the endoplasmic reticulum stress are key players in synovitis of osteoarthritis, chronic pyrophosphate arthropathy and rheumatoid arthritis, and correlate with the histological score

Dominique de Seny (1), Elettra Bianchi (2), Dominique Baiwir (3), Gaël Cobraiville (1), Charlotte Collin (1), Mégane Deliège (1), Marie-Joëlle Kaiser (1), Gabriel Mazzucchelli (4), Jean-Philippe Hauzeur (1), Philippe Delvenne (2), Michel G. Malaise (1).

Affiliation:

(1) Laboratory of Rheumatology, GIGA Research, CHU Liege, 4000 Liege, Belgium.

(2) Department of Pathology, GIGA Research, CHU Liege, 4000 Liège, Belgium

(3) GIGA Proteomics Facility, University of Liege, 4000 Liege, Belgium

(4) Mass Spectrometry Laboratory, MolSys Unit Research, University of Liege, 4000 Liege, Belgium

Corresponding author:

Dominique de Seny

Rheumatology department, Tour GIGA, +2

CHU, 4000 Liège

Belgium

office-phone : +32 4 366 24 74

e-mail : ddeseny@chuliege.be

Running Headline: Proteins of ER stress in synovitis

Conflict of interest: All authors have nothing to disclose

Abstract

Background: It is now well recognized that osteoarthritis (OA) synovial membrane presents inflammatory components. The aim of this work is to provide evidence that similar inflammatory mechanisms exist among the three pathologies presenting an inflammatory gradient: OA, chronic pyrophosphate arthropathy (CPPA) and rheumatoid arthritis (RA).

Methods: Synovial biopsies of OA (n=9), CPPA (n=7) and RA (n=8) patients were first characterized by a histological score based on synovial hyperplasia and infiltration of lymphocytes, plasma cells, polymorphonuclear and macrophages. All biopsies were also analyzed by 2D-nano-UPLC-ESI-Q-Orbitrap for protein identification and quantification. Protein levels were correlated with the histological score.

Results: Histological score was in the range of 3 to 8 for OA, 5 to 13 for CPPA and 12 to 17 for RA. Of the 4336 proteins identified by mass spectrometry, 51 proteins were selected for their strong correlation ($p<0.001$) with the histological score of which 11 proteins (DNAJB11, CALR, ERP29, GANAB, HSP90B1, HSPA1A, HSPA5, HYOU1, LMAN1, PDIA4, and TXNDC5) were involved in the endoplasmic reticulum (ER) stress. Protein levels of S100A8 and S100A9 were significantly higher in RA compared to OA (for both) or to CPPA (for S100A8 only) and also significantly correlated with the histological score. Eighteen complement component proteins were identified, but only one (complement C1q subcomponent, subunit B and C) was weakly correlated with the histological score.

Conclusions: This study highlights the inflammatory gradient existing between OA, CPPA and RA synovitis either at the protein level or at the histological level. Inflamed synovitis was characterized by the overexpression of ER stress proteins.

Key words: proteomic, synovitis, endoplasmic reticulum, biomarker, chaperone, S100A8, S100A9, complement

Abbreviation

2D-nano-UPLC-ESI-Q-Orbitrap : 2 dimensional-nano-ultra performance liquid chromatography-electrospay ionization-Q-Orbitrap

CALR: calreticulin

CPPA: chronic pyrophosphate arthropathy

CRP: C-reactive protein

DAMPS: damage-associated molecular patterns

ER: endoplasmic reticulum

ERAD: ER-associated degradation

GRP78: Glucose-Regulated Protein 78 kDa

LC-MS/MS: Liquid chromatography-tandem mass spectrometry

LFQ: label free quantitative

MRI: magnetic resonance imaging

OA: osteoarthritis

PMN: polymorphonuclear cells

RA: rheumatoid arthritis

TLR: toll-like receptors

TXNDC5: Thioredoxin domain-containing protein 5

UPR: unfolded protein response

US: ultrasonography

INTRODUCTION

Osteoarthritis (OA) was for long considered as a degenerative cartilage disease for which synovitis was only visualized in the late stages and considered as secondary to mechanic aggression of bone and cartilage degradation. However, several observations demonstrated that synovitis could appear even in the early stages of OA. Synovium can also acquire an "inflammatory" phenotype in OA with similar characteristics than those observed in rheumatoid arthritis (RA) [i.e. synovial lining and villous hyperplasia, infiltration by macrophages and lymphocytes, neo-angiogenesis and fibrosis](1,2). Using magnetic resonance imaging (MRI), Roemer *et al.* noted a synovitis in 96.3 % of knee joints with effusion and in 70 % of knee joint without effusion(3). We previously published by using ultrasonography (US) examination that 53.7% (322/600) of patients with painful knee OA had no sign of inflammation whereas 2.7% (16/600) had synovitis alone, 14.2% (85/600) had both synovitis and effusion and 29.5% (177/600) had joint effusion alone(4). US knee synovitis and US joint effusion were significantly associated with a more severe radiological grade (Kellgren-Lawrence grade $\geq$ 3) and a moderate-important joint effusion at clinical examination(4). Further, several other studies have confirmed the correlation between synovitis area observed by MRI and specific histologic features of synovitis(5).

Two major pathways at least can explain the development of synovitis: activation of toll-like receptors (TLR) and activation of the complement cascade(1). Endogenous "damage-associated molecular patterns" (DAMPS) can activate the innate immune response through TLRs recognition promoting pro-inflammatory mediators secretion(6,7).

Activation of the complement cascade induces complement deposits sparsely found in the synovium of OA patients. Deposits of synovial complement components were only observed during acute OA flare but not during chronic OA(8). More recently, proteomic

analyses of OA synovial fluids(9,10) and transcriptomic studies of OA synovial membranes(10) confirmed the expression and activation of complement in joints(11).

Proteomic analysis of synovial tissue was rarely performed(12,13) and none was compared to the histological pattern of synovium. In this work, we compared protein profiles generated by a proteomic study to the histological features of synovial biopsies obtained from patients with OA, chronic pyrophosphate arthropathy (CPPA) or RA. It unraveled an increased gradient of inflammation and synovial lining hyperplasia among the three pathologies both at the protein and histological levels.

METHODS

Patients and synovial tissue

All experiments undertaken with patient material complied with the regulations and ethical guidelines of the CHU of Liege, Belgium. Synovial biopsies of OA (n=9), CPPA (n=7) and RA patients (n=8) were obtained by needle arthroscopy from affected knees. For each patient, 3 synovial fragments were stored at -80°C until used for proteomic study. Three other fragments were also processed for formalin fixation (24 h) using a standard procedure and were embedded in paraffin for microscopic examination of the hematoxylin and eosin (H&E) stained sections and histological scoring.

Histological score

Hematoxylin eosin stained sections were scored as previously done for routine clinical analysis and randomly analyzed as described in Tak *et al*(14). Briefly, all areas of each biopsy section were examined by trained anatomopathologists (P.D. and E. B.). Histological features included synovial hyperplasia and the degree of infiltration of lymphocytes, plasma cells or polymorphonuclear cells (PMN), separately. The TAK score(14) was slightly modified: a)

synovial hyperplasia was scored on a five-point scale (0-4) instead of a four-point scale (0-3) because synovitis hallmark in RA as in OA is proliferation and hyperplasia of the lining cells(2) and b) PMN infiltration was scored on a four-point scale (0-3) instead of a five-point scale (0-4) because PMN infiltration is less intense than any other mononuclear cells infiltration. Macrophage infiltration was also determined by using immunohistochemistry with an anti-CD68 antibody [anti-CD68 (KP-1) Primary Antibody, Ventana Medical System], and the CD68 expression was scored separately using a semi-quantitative 4 scale score (0-3) with 0 for no infiltration, 1, 2 and 3 for respectively mild, moderate and severe infiltration using a pre-defined atlas(15). The histological score was determined by the sum of the components, as for other methods(14,15), leading to a maximum of 18.

LC-MS/MS analysis for proteomic analysis

The biopsies were weighted (5mg) and resuspended in 300µL of RIPA buffer in the presence of complete and phospho stop solutions. The biopsies were then disrupted using a bi-switch (+ 60mg of µbeads) for cycles of 30 sec high speed and 30 sec low speed at 4°C, during 2X15 min, to allow proteins dissolution in the buffer. The protein concentration of each sample was determined using the RCDC protein assay kit according to manufacturer recommendations (BioRad, Hercules, CA, USA). For each sample, 15µg of protein were diluted in ammonium bicarbonate (50mM) to get a protein concentration of 0.5µg/µL. The proteins were then reduced (DTT), alkylated with iodoacetamide and precipitated using the 2D clean-up kit (GE Healthcare, Belgium). The protein pellets were then resuspended in ammonium bicarbonate (50 mM) at a concentration of 0.5µg/µL and digested with trypsin. For each sample, 3.5µg of peptides were desalted using Ziptip C18 (Millipore Corp., Billerica, MA, USA) according to the manufacturer's instructions. The eluted fractions were then dried by speed-vac. Dry pellets were stored at -20°C until used for analysis. Before injection into the 2D-nano-UPLC system,

2.5µg of the digested proteins were resuspended in 9µL of 100mM ammonium formate solution adjusted to pH10. A standard MassPREP™ (MPDS mixture) digestion mixture (Waters Corp., Milford, USA) which contains a mixture of yeast enolase (ENO1, P00924), rabbit glycogen phosphorylase b (GPB, P00489), yeast alcohol dehydrogenase (ADH, P00330) and bovine serum albumin (BSA, P02769) was spiked in each sample at a quantity of 150 fmoles of ADH digest per injection.

All samples were injected on a 2D-nanoAquity UPLC (Waters, Corp., Milford, USA) coupled online with a ESI-Q-Orbitrap (Q Exactive, Thermo Fisher Scientific) in positive ion mode. Briefly, the liquid chromatography approach used was a 2-dimensional method (2D-LC) comprising 3 steps of 180 min. The 3 steps were carried out on a high pH column with increasing percentage of acetonitrile. The eluted peptides were then injected onto a low pH column for which each step consists of a 5min gradient from 99% buffer A (A = H_2O, 0.1% formic acid, B = acetonitrile) to 93% of A followed by a gradient of 135min from 93% of A to 65% of A. The acquisition method was a TopN-MSMS where N was set to 12, meaning that the spectrometer acquired one Full MS spectrum, selected the 12 most intense peaks in this spectrum (singly charged precursors excluded) and recorded a Full MS2 spectrum of each of these 12 compounds. The parameters for MS spectrum acquisition were: mass range from 400 to 1750 *m/z*, resolution of 70000, automated gain control (AGC) target of 10^6 or maximum injection time of 200ms. The parameters for MS2 spectrum acquisition were: isolation window of 2.0 *m/z*, collision energy (NCE) of 25, resolution of 17500, AGC target of 10^5 or maximum injection time of 50ms. The database searches were performed by the software MaxQuant ver.1.5.2.8. Protein identifications were considered as significant if these proteins were identified with at least 2 peptides including at least one unique peptide per protein considering a false positive discovery rate (FDR) <0.01.

Data analysis

Epidemiological data of the 3 groups (OA, CPPA and RA) were compared using the Kruskal Wallis test with the posthoc test of Dunn's for continuous variables and Chi square test for qualitative variables. Comparison of two-by-two groups for K&L was performed with Mann Whitney test.

For MS/MS values, Maxquant analysis leads to the identification and calculation of the normalized protein intensities. The label free quantitative (LFQ) intensities can be directly compared between samples (for a given protein) and can be imported in Perseus software (version 1.5.5.0) for statistical differential analysis. Only proteins identified in 7 biopsies of at least one of the three groups (OA, CPPA and RA) were considered for further analysis. 1871 proteins were selected accordingly. LFQ intensities were Log2 transformed for all statistical analyses. Correlation coefficients were obtained using Pearson test after verifying that all values passed the D'Agostino normality test. Multiple-comparison test (ANOVA) was used for comparing protein intensities of the three groups [OA, CPPA and RA]. DAVID Bioinformatics resources 6.8 was used for the identification of KEGG pathways. STRING 10.5 was used for functional protein association network.

RESULTS

Characteristics of patients

Clinical and biologic data are summarized in Table 1. Parameters related to age, gender and BMI were not statistically different between OA, CPPA and RA patients. Severity of OA and CPPA was defined according to the Kellgren Lauwrence (K&L) grade(16) and was not statistically different between the two groups. Histological score was significantly different between the 3 groups (P value = 0.0003) and was higher in RA compared to OA ($P<0.001$) or

CPPA ($P<0.05$) but not different between OA and CPPA groups according to the posthoc test. CRP values exceeding the normal range were observed in 20%, 40% and 90% of OA, CPPA and RA patients, respectively; all patients being untreated by corticosteroids or any disease modifying anti-rheumatic drugs, including biologics.

Histological score

Histological score was in the range of 3 to 8 for OA, 5 to 13 for CPPA and 12 to 17 for RA, which represents a continuum for the inflammatory process of the synovial membrane through the 24 biopsies, the least severe being the OA group in contrast to CPPA (medium score) and RA (highest score) (Table 1, Figure 1A). Of note, there is an overlap between the 3 pathologies, and some patients with OA have already a medium high inflammatory score. Synovial hyperplasia and infiltration of lymphocytes were observed in all samples (Figure 1A and 1B), whereas plasmocytic infiltration was observed in only 3/9 OA (33%), 3/7 (43%) CPPA and 8/8 RA synovitis, and PMN infiltration in 0/9 OA, in 1/7 (14%) CPPA and in 6/8 (75%) RA synovitis (Figure 1A and 1B). Macrophage infiltration was present in 8/9 (89%) of OA, in 5/7 (71%) of CPPA and in 8/8 RA synovitis (Figure 1A and 1C).

Proteomics analysis

Proteins were extracted and digested from the 24 biopsies for proteomic analysis by mass spectrometry (MS/MS). 4336 proteins were identified by MS/MS, but only 1871 proteins were selected for their significant identification in 7 biopsies of at least one of the three groups (OA, CPPA or RA). The 1871 proteins intensities were then correlated with their corresponding histological score. Fifty-one proteins presented a statistically significant correlation with a P value being at least <0.001 (Table 2), including 39 proteins with a positive correlation ($r >0.63$) and 12 proteins with a negative correlation ($r<-0.65$) (Table 2). Some proteins of Table 2 are

illustrated in Figure 2 for the three groups, as well as correlation parameters between MS/MS log2 protein intensities and respective histological score. Highlighted grey lines of Table 2 feature 31 proteins detected in the entire set of the 24 biopsies, including 27 proteins being positively correlated with the histological score and 4 proteins being negatively correlated (Table 2).

We also confirmed that DAMP proteins, S100A8 and S100A9, were detected in the 24 synovial membrane biopsies and that their protein levels were strongly increased in RA compared to OA biopsies (ANOVA, Tuckey post hoc test $P<0.01$). Only S100A8 but not S100A9 protein levels were discriminant between CPPA and RA groups ($P<0.01$). As expected, a strong correlation between S100A8 and S100A9 protein levels ($r=0.95$, $P<0.0001$) was determined among the 3 groups.

DAVID analysis was performed on the 51 biomarkers to highlight their functional classifications (Figure 3A). The pathway entitled "protein processing in endoplasmic reticulum (ER)" was selected and weighted in the balance for 22% (Figure 3A). In this pathway, 11 proteins were identified: *DNAJB11*, *CALR*, *ERP29*, *GANAB, HSP90B1*, *HSPA1A*, *HSPA5*, *HYOU1*, *LMAN1*, *PDIA4*, and *TXNDC5* (Figure 3B) and were connected by the STRING protein-protein interaction network (see red writings in Figure 3C). Statistically significant positive correlations were confirmed and summarized in Figure 3D, except for *HSPA1A* that was negatively correlated to the 10 others. Out of that observation, we calculated the ratio of *HSPA1A* to *TXNDC5* protein levels that was negatively correlated ($r=-0.6$, $P=0.002$) with the histological score (Figure 3E). Although DAVID analysis did not highlight a pathway centered on the alarmins S100A8 and S100A9, both proteins were significantly correlated with almost all 50 other proteins selected in Table 2, except for *PARP1* and *CRTAC1* for S100A8 or S100A9, and *GANAB* and *GNB2L1* for S100A9 (Table 3). The same 39 proteins as in Table 2

were positively correlated with S100A8 or S100A9, as well as the 12 proteins that were negatively correlated (Table 3).

A special attention was drawn to the status of complement component protein levels: 18 have been identified among the 1871 proteins retained (Additional file 1). Only complement C1q subunits B and C were slightly significantly correlated with the histological score.

DISCUSSION

OA synovitis share at a lower degree many common features with RA synovitis including abnormal synoviocytes proliferation, leukocytes infiltration and angiogenesis. In our study, synovial hyperplasia and lymphocyte infiltration were observed in all samples. Macrophages infiltration was detected in all biopsies except for 2 OA and 1 CPPA synovitis. Plasmocytes infiltration was observed in all RA and in 33-43% of non-RA biopsies, whereas PMN infiltration was present in 75% of RA biopsies and in 0-10% of non-RA biopsies. The histological score highlighted an inflammatory continuum through the 24 biopsies with an overlap between the 3 studied pathologies in agreement with other publications(1,2,15). It emphasizes the absence of a unique pattern for each studied disease and the heterogeneity of cell infiltration, either quantitatively and qualitatively. Synovitis is composed of various inflammatory cells and proliferating synoviocytes that induce the secretion of classical inflammatory mediators but also the secretion of thousands of proteins that represents the dark proteome, a Gordian knot that can only be unraveled by a tissue proteomic analysis.

To the best of our knowledge, this is the first proteomic study of human synovitis for which proteins levels were compared to their corresponding histological score. DAVID and STRING analyses highlighted 11 proteins involved in the endoplasmic reticulum pathway: *DNAJB11*, *CALR*, *ERP29*, *GANAB*, *HSP90B1*, *HSPA1A*, *HSPA5*, *HYOU1*, *LMAN1*, *PDIA4*, and *TXNDC5*. All these proteins were detected in the 24 biopsies supporting the relevance of

their identifications. How can we connect ER proteins to the inflammatory process inside synovitis? Endoplasmic reticulum (ER) is an intracellular organelle playing a major role in proper proteins folding through the activation of several chaperone proteins, including protein disulfide isomerase (PDI), ERP29, the Hsp70 family member Glucose-Regulated Protein 78 kDa (GRP78/BiP) (*HSPA5*), and calreticulin (*CALR*). However, despite the function of these chaperones, the success rate for proper folding is often quite low. Incompletely folded proteins are forced to be removed from cells by a process called UPR (unfolded protein response) activated along with the ER-associated degradation (ERAD), enhancing protein degradation by the proteasome. Some cellular disturbances such as nutrient deprivation, hypoxia or loss of calcium homeostasis can disrupt ER efficiency and lead to the accumulation of unfolded proteins enhancing a stress response in the ER.

Under normal conditions, GRP78/BiP (*HSPA5*) maintains the canonical UPR regulators (IRE1α, PERK and ATF6) in an inactivated form, while upon pathological conditions, it dissociates from the three UPR proteins inducing UPR activation(17). Contribution of the ER stress in RA pathogenesis has been recently described(17). Inflammation and ER stress work together by driving inflammatory cells to produce pro-inflammatory cytokines but also to enhance FLS proliferation and angiogenesis(17,18). Further, synovial hyperplasia is linked to chronic inflammation and joint destruction(1). GRP78/BiP has been localized predominantly in the lining but also sublining layers of RA (more pronounced) and OA synovium(18). Down-regulation of GRP78/BiP increases apoptosis of RA FLS and conversely its overexpression prevents cells from apoptotic death induced by an ER stressor(18). Selective abrogation of GRP78/BiP blunts activation of NF-κB and protect mice from collagen arthritis(19).

ERdj3 (*DNAJB11*) acts as a component with other co-chaperone proteins SDF2 and SDF2L1 in the GRP78/BiP chaperone cycle to prevent the aggregation of misfolded proteins(20) and regulates GRP78/BiP occupancy in living cells(21). Two other ER

chaperones, such as GRP94/endoplasmin (*HSP90B1*) and calreticulin (*CALR*) contribute to the autoimmune process in different ways. Under physiologic conditions, GRP94/endoplasmin optimizes the function of B cells by chaperoning TLRs(22). Indeed, GRP94/endoplasmin ablation in B cells attenuated antibody production in the context of TLR stimulation(22). Under pathologic conditions, GRP94/endoplasmin translocates to the cell surface and extracellular space and could function as an autoantigen to induce autoantibodies and enhance immune responses(23). GRP94/endoplasmin may also act as an endogenous ligand of TLR2 to promote chronic inflammation(23). GRP94/endoplasmin induces the transcription of TLR2, TNF-α and IL8 but not TLR4 in synovial macrophages(24). GRP94/endoplasmin is highly expressed in the lining and sublining layers of RA synovium correlating with lining thickness (lining) and the inflammatory score (sublining)(24). Its expression was also detected in control OA synovium(24). A recent study demonstrated that the upregulation of Bcl-XL and Mcl-1 expression in RA FLS by calreticulin promoted apoptosis resistance of RA FLS(25). Calreticulin promotes angiogenesis by activating nitric oxide signaling pathway in RA(26). Further, soluble calreticulin can induce the expression of pro-inflammatory cytokines by macrophages(27). Calreticulin was previously detected by another proteomic study focusing on formalin-fixed paraffin-embedded (FFPE) synovial tissues provided from OA and RA tissues(12).

Hypoxia-upregulated protein 1 (*HYOU1*) or GRP170 is co-regulated and associated with two other chaperones GRP78/BiP and GRP94/endoplasmin, suggesting their coordinated activity in the maintenance of protein homeostasis(28). HYOU1 presents an important cytoprotective role in hypoxia-induced cellular perturbation(29) and can contribute to cell survival when ER is under stress. However, surface or extracellular HYOU1 exerts documented immunoregulatory activities in some immunopathologies but its role in rheumatic diseases remains unknown(30). In addition to its function as a “danger” molecule alerting the immune

system of tissue damage, the extracellular HYOU1 has also the capacity of amplifying the inflammatory response triggered by microbial signals and possibly by DAMPs(30). HYOU1 also promoted pulmonary fibrosis in mice by increasing pulmonary levels of TGF-β1 and myofibroblasts(31).

Thioredoxin domain-containing protein 5 (*TXNDC5*) is a protein disulfide isomerase with clear pro-inflammatory properties. TXNDC5 contributes to abnormal RA FLS proliferation, migration and IL-6 production by inhibiting IGFBP1 expression(32). Downregulation of TXNDC5 could contribute to RA FLS antiangiogenic and proapoptotic features through the suppression of CXCL10 and TRAIL(33). Further, TXNDC5 synergizes with heat shock cognate 70 protein (HSC70) to exacerbate the inflammatory phenotype of RA FLS through NF-κB signaling(34). TXNDC5 expression was increased in synovial tissues of RA patients compared to OA as identified by a proteomic study(13) or by immunochemistry(35). Further, elevated levels were found in the synovial fluid and serum of RA patients(35).

The role of ERp29 (*ERP29*) seems controversial in the literature regarding to apoptosis. It protects cells such as neurons from apoptosis(36) whereas it sensitizes some others such as cancer cells(37). Murine macrophages upon interaction with heat-inactivated Candida albicans unravel an anti-inflammatory response with the overexpression of ERp29(38). Protein disulfide-isomerase-A4 (PDIA4) mediates resistance to cisplatin-induced cell death in lung adenocarcinoma(39). PDIA4 mRNAs were significantly increased in patients' inflamed colonic mucosa compared to uninflamed mucosa and controls(40). Protein ERGIC-53 (*LMAN1*) is a type I transmembrane protein that is located at the ER, ER-Golgi Intermediate Compartment (ERGIC) and cis-Golgi. Protein ERGIC-53 facilitates transport of several cargo proteins including factors critical to the coagulation cascade from the ER to Golgi(41). Interaction of Protein ERGIC-53 with β-amyloid protected cultured neuronal cells from β-amyloid-induced

apoptosis(42). GANAB is a key glycoprotein quality control protein in ER removing glucose residues from immature glycoproteins(43). Although ERp29, PDIA4, Protein ERGIC-53 and GANAB proteins were highly positively correlated in our work with the histological score, their presence and their role in the pathophysiology of synovitis have not yet been described.

As for other chaperones, the heat shock 70 kDa protein 1A/1B or Hsp72 (*HSPA1A*) can be released by normal cell under stress or by damaged cell, but unlike most of other chaperones, HSPA1A displays anti-inflammatory properties. Recombinant human HSPA1A suppresses the production of pro-inflammatory cytokines in RA FLS by inhibition of NF-κB pathway and decreases collagen-induced arthritis in mice(44). Interestingly, in our study, HSPA1A levels were significantly lower in RA than in OA or CPPA synovium and negatively correlated with the histological score as well as with the 10 other aforementioned protein levels of the ER pathway suggesting a defective anti-inflammatory response in favor of a pro-inflammatory one under the control of ER proteins.

S100A8 and S100A9 were expressed in the 24 biopsies and positively correlated with the histological score. Further, they were almost correlated to all 51 proteins highlighted for their correlation with the histological score. S100A8 and S100A9 proteins are Ca2+ binding proteins constitutively expressed by neutrophils and monocytes. They are well-known DAMPs proteins participating to leukocyte recruitment and cytokines secretion and are highly expressed in many inflammatory conditions. They were detected in serum(45), synovial fluid(46) and joint tissue(12,13) of RA patients. In the OA synovium, they are mainly produced by M-1 like macrophages and slightly by M-2 like macrophages but not by FLS, inducing inflammatory cytokines and MMPs expression(47). S100A8 and S100A9 are actively involved in the thickening of the intimal layer and in the development of joint destruction in murine collagenase-induced OA but not in destabilized medial meniscus-induced OA(48). Further, S100A8 and S100A9 levels in the OA synovitis significantly correlate with synovial lining

thickness and cellularity in the subintima(48). Gene and protein expression of S100A9 were increased in inflamed areas as compared to normal area of human OA synovitis(49).

Eighteen complement component proteins were identified but none except complement C1q was positively correlated to the histological score. These findings are in contrast with two other proteomic analyses(9,10) performed in OA synovial fluids but not in tissue. Indeed, Gobezie *et al.* identified C3 as a discriminant marker exhibiting a sensitivity of 90% and a specificity of 85% in OA synovial fluids(9). Similarly, we also identified previously increased levels of C3f fragment in synovial fluid of OA patients (11). Complement components can be delivered from blood by ultrafiltration. Numerous publications mentioned that complement components could be produced by synovial tissue cells(50). However, in our study, complement component levels in OA, CPPA and RA were not correlated to the histological score and were not statistically elevated among the three pathologies, suggesting that complement cascade was further playing a role in synovial fluids and not in synovial tissue.

CONCLUSION

This study highlights the continuum existing between OA, CPPA and RA synovitis both at the protein and the histological score levels. These two levels are connected giving pathophysiological relevance of the proteomic synovium analysis. Pannus development in these diseases is characterized by overexpression of many proteins involved in the ER stress, mostly chaperones and co-chaperones. All studied ER proteins except HSPA1A exhibit pro-inflammatory properties when they are exposed on the cell membrane or secreted outside favoring inflammatory cytokine production as well as proliferation and migration of FLS. Five proteins (*HSPA5, HSB90B1, CALR, TXNDC5* and *HSPA1A*) have been previously identified in the RA synovium and to a lesser extent in the OA synovium. Six proteins (*DNAJB11, HYOUI, ERp29, PDIA4, LMAN1 and GANAB*) have never been described in RA or in OA synovium,

and none in CPPA synovium. These data confirm an important role for these chaperones and co-chaperones of the ER pathway in the pathophysiology of RA, but more importantly strongly suggest a similar unknown pattern in the pathophysiology of OA and CPPA. S100A8 and S100A9 were correlated to the histological score and to most of highlighted proteins in Table 2. Complement components seem to behave independently from the histological score. We have also highlighted the negative correlation between the histological score and the HSPA1A/TXNDC5 ratio, which fits with the capacity of TXNDC5 to exacerbate the inflammatory phenotype of FLS(34). This proteomic analysis suggests the need for future developments such as: 1) the identification of other pathways including other proteins that are not correlated with the histological score, and 2) the characterization of protein clusters correlated with each type of cells infiltrating the pannus as well as with FLS proliferative capacity. This tool may allow to develop a molecular classification of complex rheumatic diseases.

DECLARATIONS

Ethics approval and consent to participate

All experiments undertaken with patient material complied with the regulations and ethical guidelines of the CHU of Liege, Belgium.

Consent for publication: Not applicable

Availability of data and materials: The datasets used and/or analyzed during the current study are available from the corresponding author on reasonable request.

Competing interests: We declare that we have no competing of interest.

Funding: This study was supported by the "Fond d'Investissement pour la Recherche Scientifique" (FIRS), CHU Liège, Belgium.

Authors' contributions:

All authors were involved in drafting and revision of the manuscript and all authors approved the final version to be published.

Study conception and design: de Seny D, Malaise MG

Acquisition of data: Bianchi E, Baiwir D, Cobraiville G, Collin C, Deliège M, Kaiser MJ, Mazzucchelli G, Hauzeur JP

Analysis and interpretation of data: de Seny D, Delvenne P, Malaise MG

Acknowledgements: We thank the GIGA Proteomics Facility, ULiege.

REFERENCES

1. Scanzello CR, Goldring SR. The role of synovitis in osteoarthritis pathogenesis. Bone. 2012 Aug;51(2):249–57.
2. Mathiessen A, Conaghan PG. Synovitis in osteoarthritis: current understanding with therapeutic implications. Arthritis Res Ther. 2017 Feb 2;19(1):18.
3. Roemer FW, Kassim Javaid M, Guermazi A, Thomas M, Kiran A, Keen R, et al. Anatomical distribution of synovitis in knee osteoarthritis and its association with joint effusion assessed on non-enhanced and contrast-enhanced MRI. Osteoarthr Cartil. 2010 Oct;18(10):1269–74.
4. D'Agostino MA, Conaghan P, Le Bars M, Baron G, Grassi W, Martin-Mola E, et al. EULAR report on the use of ultrasonography in painful knee osteoarthritis. Part 1: prevalence of inflammation in osteoarthritis. Ann Rheum Dis. 2005 Dec;64(12):1703–9.
5. Liu L, Ishijima M, Futami I, Kaneko H, Kubota M, Kawasaki T, et al. Correlation between synovitis detected on enhanced-magnetic resonance imaging and a histological

analysis with a patient-oriented outcome measure for Japanese patients with end-stage knee osteoarthritis receiving joint replacement surgery. Clin Rheumatol. 2010 Oct;29(10):1185–90.

6. Gómez R, Villalvilla A, Largo R, Gualillo O, Herrero-Beaumont G. TLR4 signalling in osteoarthritis-finding targets for candidate DMOADs. Nat Rev Rheumatol. 2015 Mar 16;11(3):159–70.

7. de Seny D, Cobraiville G, Charlier E, Neuville S, Esser N, Malaise D, et al. Acute-phase serum amyloid a in osteoarthritis: regulatory mechanism and proinflammatory properties. PLoS One. 2013;8(6):e66769.

8. Konttinen YT, Ceponis A, Meri S, Vuorikoski A, Kortekangas P, Sorsa T, et al. Complement in acute and chronic arthritides: assessment of C3c, C9, and protectin (CD59) in synovial membrane. Ann Rheum Dis. 1996 Dec;55(12):888–94.

9. Gobezie R, Kho A, Krastins B, Sarracino DA, Thornhill TS, Chase M, et al. High abundance synovial fluid proteome: distinct profiles in health and osteoarthritis. Arthritis Res Ther. 2007;9(2):R36.

10. Ritter SY, Subbaiah R, Bebek G, Crish J, Scanzello CR, Krastins B, et al. Proteomic analysis of synovial fluid from the osteoarthritic knee: comparison with transcriptome analyses of joint tissues. Arthritis Rheum. 2013 Apr;65(4):981–92.

11. de Seny D, Sharif M, Fillet M, Cobraiville G, Meuwis M-A, Marée R, et al. Discovery and biochemical characterisation of four novel biomarkers for osteoarthritis. Ann Rheum Dis. 2011 Jun;70(6):1144–52.

12. Hayashi J, Kihara M, Kato H, Nishimura T. A proteomic profile of synoviocyte lesions microdissected from formalin-fixed paraffin-embedded synovial tissues of rheumatoid arthritis. Clin Proteomics. 2015;12(1):20.

13. Chang X, Cui Y, Zong M, Zhao Y, Yan X, Chen Y, et al. Identification of proteins with

increased expression in rheumatoid arthritis synovial tissues. J Rheumatol. 2009 May;36(5):872–80.

14. Tak PP, Thurkow EW, Daha MR, Kluin PM, Smeets TJM, Meinders AE, et al. Expression of adhesion molecules in early rheumatoid synovial tissue. Clin Immunol Immunopathol. 1995 Dec;77(3):236–42.

15. Najm A, le Goff B, Venet G, Garraud T, Amiaud J, Biha N, et al. IMSYC immunologic synovitis score: A new score for synovial membrane characterization in inflammatory and non-inflammatory arthritis. Joint Bone Spine [Internet]. 2019 Jan;86(1):77–81.

16. Kellgren JH, Lawrence JS. Radiological assessment of osteo-arthrosis. Ann Rheum Dis. 1957 Dec;16(4):494–502.

17. Rahmati M, Moosavi MA, McDermott MF. ER Stress: A Therapeutic Target in Rheumatoid Arthritis? Trends Pharmacol Sci. 2018;39(7):610–23.

18. Yoo S-A, You S, Yoon H-J, Kim D-H, Kim H-S, Lee K, et al. A novel pathogenic role of the ER chaperone GRP78/BiP in rheumatoid arthritis. J Exp Med. 2012 Apr 9;209(4):871–86.

19. Nakajima S, Hiramatsu N, Hayakawa K, Saito Y, Kato H, Huang T, et al. Selective abrogation of BiP/GRP78 blunts activation of NF-κB through the ATF6 branch of the UPR: involvement of C/EBPβ and mTOR-dependent dephosphorylation of Akt. Mol Cell Biol. 2011 Apr;31(8):1710–8.

20. Fujimori T, Suno R, Iemura S-I, Natsume T, Wada I, Hosokawa N. Endoplasmic reticulum proteins SDF2 and SDF2L1 act as components of the BiP chaperone cycle to prevent protein aggregation. Genes Cells. 2017 Aug;22(8):684–98.

21. Guo F, Snapp EL. ERdj3 regulates BiP occupancy in living cells. J Cell Sci. 2013 Mar 15;126(Pt 6):1429–39.

22. Liu B, Li Z. Endoplasmic reticulum HSP90b1 (gp96, grp94) optimizes B-cell function

via chaperoning integrin and TLR but not immunoglobulin. Blood. 2008 Aug 15;112(4):1223–30.

23. Huang Q-Q, Pope RM. The role of glycoprotein 96 in the persistent inflammation of rheumatoid arthritis. Arch Biochem Biophys. 2013 Feb 1;530(1):1–6.

24. Huang Q-Q, Sobkoviak R, Jockheck-Clark AR, Shi B, Mandelin AM, Tak PP, et al. Heat shock protein 96 is elevated in rheumatoid arthritis and activates macrophages primarily via TLR2 signaling. J Immunol. 2009 Apr 15;182(8):4965–73.

25. Jiao Y, Ding H, Huang S, Liu Y, Sun X, Wei W, et al. Bcl-XL and Mcl-1 upregulation by calreticulin promotes apoptosis resistance of fibroblast-like synoviocytes via activation of PI3K/Akt and STAT3 pathways in rheumatoid arthritis. Clin Exp Rheumatol. 2018;36(5):841–9.

26. Ding H, Hong C, Wang Y, Liu J, Zhang N, Shen C, et al. Calreticulin promotes angiogenesis via activating nitric oxide signalling pathway in rheumatoid arthritis. Clin Exp Immunol. 2014 Nov;178(2):236–44.

27. Duo C-C, Gong F-Y, He X-Y, Li Y-M, Wang J, Zhang J-P, et al. Soluble calreticulin induces tumor necrosis factor-α (TNF-α) and interleukin (IL)-6 production by macrophages through mitogen-activated protein kinase (MAPK) and NFκB signaling pathways. Int J Mol Sci. 2014 Feb 20;15(2):2916–28.

28. Lin HY, Masso-Welch P, Di YP, Cai JW, Shen JW, Subjeck JR. The 170-kDa glucose-regulated stress protein is an endoplasmic reticulum protein that binds immunoglobulin. Mol Biol Cell. 1993 Nov;4(11):1109–19.

29. Ozawa K, Kuwabara K, Tamatani M, Takatsuji K, Tsukamoto Y, Kaneda S, et al. 150-kDa oxygen-regulated protein (ORP150) suppresses hypoxia-induced apoptotic cell death. J Biol Chem. 1999 Mar 5;274(10):6397–404.

30. Zuo D, Subjeck J, Wang X-Y. Unfolding the Role of Large Heat Shock Proteins: New

Insights and Therapeutic Implications. Front Immunol. 2016;7(MAR):75.

31. Tanaka K, Shirai A, Ito Y, Namba T, Tahara K, Yamakawa N, et al. Expression of 150-kDa oxygen-regulated protein (ORP150) stimulates bleomycin-induced pulmonary fibrosis and dysfunction in mice. Biochem Biophys Res Commun. 2012 Sep 7;425(4):818–24.

32. Li J, Xu B, Wu C, Yan X, Zhang L, Chang X. TXNDC5 contributes to rheumatoid arthritis by down-regulating IGFBP1 expression. Clin Exp Immunol. 2018;192(1):82–94.

33. Xu B, Li J, Wu C, Liu C, Yan X, Chang X. CXCL10 and TRAIL Are Upregulated by TXNDC5 in Rheumatoid Arthritis Fibroblast-like Synoviocytes. J Rheumatol. 2018 Mar;45(3):335–40.

34. Wang L, Dong H, Song G, Zhang R, Pan J, Han J. TXNDC5 synergizes with HSC70 to exacerbate the inflammatory phenotype of synovial fibroblasts in rheumatoid arthritis through NF-κB signaling. Cell Mol Immunol. 2018;15(7):685–96.

35. Chang X, Zhao Y, Yan X, Pan J, Fang K, Wang L. Investigating a pathogenic role for TXNDC5 in rheumatoid arthritis. Arthritis Res Ther. 2011 Jul 29;13(4):R124.

36. Zhang Y-H, Belegu V, Zou Y, Wang F, Qian B-J, Liu R, et al. Endoplasmic Reticulum Protein 29 Protects Axotomized Neurons from Apoptosis and Promotes Neuronal Regeneration Associated with Erk Signal. Mol Neurobiol. 2015 Aug;52(1):522–32.

37. Zhang D, Richardson DR. Endoplasmic reticulum protein 29 (ERp29): An emerging role in cancer. Int J Biochem Cell Biol. 2011 Jan;43(1):33–6.

38. Martínez-Solano L, Reales-Calderón JA, Nombela C, Molero G, Gil C. Proteomics of RAW 264.7 macrophages upon interaction with heat-inactivated Candida albicans cells unravel an anti-inflammatory response. Proteomics. 2009 Jun;9(11):2995–3010.

39. Tufo G, Jones AWE, Wang Z, Hamelin J, Tajeddine N, Esposti DD, et al. The protein

disulfide isomerases PDIA4 and PDIA6 mediate resistance to cisplatin-induced cell death in lung adenocarcinoma. Cell Death Differ. 2014 May;21(5):685–95.

40. Negroni A, Prete E, Vitali R, Cesi V, Aloi M, Civitelli F, et al. Endoplasmic reticulum stress and unfolded protein response are involved in paediatric inflammatory bowel disease. Dig Liver Dis. 2014 Sep;46(9):788–94.

41. Zhang B, Kaufman RJ, Ginsburg D. LMAN1 and MCFD2 form a cargo receptor complex and interact with coagulation factor VIII in the early secretory pathway. J Biol Chem. 2005 Jul 8;280(27):25881–6.

42. Nelson TJ, Alkon DL. Protection against beta-amyloid-induced apoptosis by peptides interacting with beta-amyloid. J Biol Chem. 2007 Oct 26;282(43):31238–49.

43. Pelletier MF, Marcil A, Sevigny G, Jakob CA, Tessier DC, Chevet E, et al. The heterodimeric structure of glucosidase II is required for its activity, solubility, and localization in vivo. Glycobiology. 2000;10(8):815–27.

44. Luo X, Zuo X, Mo X, Zhou Y, Xiao X. Treatment with recombinant Hsp72 suppresses collagen-induced arthritis in mice. Inflammation. 2011 Oct;34(5):432–9.

45. de Seny D, Fillet M, Ribbens C, Marée R, Meuwis M-A, Lutteri L, et al. Monomeric calgranulins measured by SELDI-TOF mass spectrometry and calprotectin measured by ELISA as biomarkers in arthritis. Clin Chem. 2008 Jun;54(6):1066–75.

46. Baillet A. [S100A8, S100A9 and S100A12 proteins in rheumatoid arthritis]. La Rev Med interne. 2010 Jun;31(6):458–61.

47. van den Bosch MH, Blom AB, Schelbergen RF, Koenders MI, van de Loo FA, van den Berg WB, et al. Alarmin S100A9 Induces Proinflammatory and Catabolic Effects Predominantly in the M1 Macrophages of Human Osteoarthritic Synovium. J Rheumatol. 2016 Oct;43(10):1874–84.

48. van Lent PLEM, Blom AB, Schelbergen RFP, Slöetjes A, Lafeber FPJG, Lems WF, et

al. Active involvement of alarmins S100A8 and S100A9 in the regulation of synovial activation and joint destruction during mouse and human osteoarthritis. Arthritis Rheum. 2012 May;64(5):1466–76.

49. Lambert C, Dubuc J-E, Montell E, Vergés J, Munaut C, Noël A, et al. Gene expression pattern of cells from inflamed and normal areas of osteoarthritis synovial membrane. Arthritis Rheumatol (Hoboken, NJ). 2014 Apr;66(4):960–8.

50. Neumann E, Barnum SR, Tarner IH, Echols J, Fleck M, Judex M, et al. Local production of complement proteins in rheumatoid arthritis synovium. Arthritis Rheum. 2002 Apr;46(4):934–45.

FIGURE LEGENDS

Figure 1: Histological scoring of synovial biopsies A) Classification of OA, CPPA and RA synovial biopsies (n = 24) according to the histological score based on the following criteria: synovial hyperplasia (hs, 0 – 4), infiltration of lymphocytes (ly, 0 – 4), plasmocytes (pl, 0 – 4), polynuclear neutrophils (po, 0 – 3) and macrophages (CD68, 0 – 3). B) Histological representation of hematoxylin eosin stained sections for synovial hyperplasia and infiltration of lymphocytes/plasmocytes and polynuclear neutrophils in one OA, CPPA or RA biopsy. C) Immunohistochemistry using anti-CD68 antibody showing macrophage infiltration in OA, CPPA and RA synovial biopsies.

Figure 2: Distribution of protein intensities among the 3 groups (OA, CPPA and RA) and correlation with the histological score

Illustration of some proteins from Table 2 for which log2 intensities obtained by MS/MS are represented among the three groups (OA, CPPA and RA) and statistically correlated to the histological score.

Figure 3: ER stress proteins detected in the inflamed synovial membrane: A) DAVID analysis performed on the 51 biomarkers highlighted for their significant correlation to the histological score, for their functional classifications. The pathway entitled "protein processing in endoplasmic reticulum (ER)" was selected. B) Proteins involved in the ER pathway according to DAVID analysis. C) STRING protein-protein interaction among the 51 proteins highlighted in Table 2. Red writings indicate proteins involved in the ER network according to DAVID analysis. D) Correlation parameters between the 11 proteins involved in the ER according to DAVID. E) Negative correlation between HSPA1A and TXNDC5 protein levels.

Additional file 1: Correlation parameters between complement components and the histological score

Representation of complement components intensities obtained by MS/MS among the three groups (OA, CPPA and RA). * represent P-values < 0.05; ns = not significant

Table 1: Patients description

Clinical and pathological characteristics of patients with osteoarthritis (OA), chronic pyrophosphate arthropathy (CPPA) or rheumatoid arthritis (RA)

	OA	CPPA	RA	P value
n	9	7	8	
Age [median (interval)]	55 (36-89)	65 (50-74)	57 (29-78)	0.3
% of woman	88% (8/9)	71% (5/7)	62% (5/8)	0.44
BMI [median (interval)]	32.2 (17.6-41.9)	24.2 (22-33)	24.4 (16.4-33.9)	0.4
K&L score [median (interval)]	3 (0-4)	2 (0-4)	/	0.6
Histological inflammatory score	4 (3-8)	5 (5-13)	14 (12-17)	0.0003
Anti-CCP (positive %)	0%	0%	60%	0.002
Rheumatoid factor (positive %)	0%	0%	40%	0.032
CRP (Positive %)	20%	40%	90%	0.020
ESR (Positive %)	10%	0%	60%	0.01

OA = osteoarthritis; CPPA = chronic pyrophosphate arthropathy; RA = rheumatoid arthritis;
BMI = Body mass index; K&L = Kellgren and Lauwrence score;
anti-CCP = anti-cyclic citrullinated peptide; CRP = C reactive protein; ESR = erythrocyte sedimentation rate

Table 2: Correlation parameters between protein intensities and histological score

Intensities of 51 proteins quantified by MS/MS were significantly correlated to the histological score. n = number of biopsies for which the protein was detected; r = coefficient correlation (Pearson test). P-values are statistically significant < 0.001.

Gene ID	Prot ID	Prot name	n	r	P-value
LSP1	P33241	Lymphocyte-specific protein 1	16	0.83	< 0.0001
MZB1	Q8WU39	Marginal zone B- and B1-cell-specific protein	15	0.80	0.0004
MANF	P55145	Mesencephalic astrocyte-derived neurotrophic factor	23	0.79	< 0.0001
EML4	Q9HC35	Echinoderm microtubule-associated protein-like 4	20	0.78	< 0.0001
LAP3	P28838	Cytosol aminopeptidase	24	0.77	< 0.0001
DNAJB11	Q9UBS4	DnaJ homolog subfamily B member 11	24	0.77	< 0.0001
DEFA1	P59665	Neutrophil defensin 1	21	0.76	< 0.0001
ERP29	P30040	Endoplasmic reticulum resident protein 29	24	0.75	< 0.0001
IDH2	P48735	Isocitrate dehydrogenase [NADP], mitochondrial	24	0.75	< 0.0001
LCP1	P13796	Plastin-2	24	0.74	< 0.0001
TXNDC5	Q8NBS9	Thioredoxin domain-containing protein 5	24	0.73	< 0.0001
HSP90B1	P14625	Endoplasmin or glucose-related protein 94 (GRP94)	24	0.73	< 0.0001
CALR	P27797	Calreticulin	24	0.73	< 0.0001
PRDX4	Q13162	Peroxiredoxin-4	24	0.73	< 0.0001
SRP72	O76094	Signal recognition particle subunit SRP72	22	0.73	0.0001
HSPA5	P11021	78 kDa glucose-regulated protein (GRP78) or BiP	24	0.72	< 0.0001
ARHGDIB	P52566	Rho GDP-dissociation inhibitor 2	24	0.72	< 0.0001
PDIA4	P13667	Protein disulfide-isomerase A4	24	0.72	< 0.0001
TAPBP	O15533	Tapasin	18	0.72	0.0009
CORO1A	P31146	Coronin-1A	24	0.71	< 0.0001
S100A8	P05109	Protein S100-A8	24	0.71	0.0001
CTSS	P25774	Cathepsin S	22	0.69	0.0003
CTSZ	Q9UBR2	Cathepsin Z	24	0.69	0.0002
MNDA	P41218	Myeloid cell nuclear differentiation antigen	23	0.69	0.0003
LMNB1	P20700	Lamin-B1	24	0.69	0.0002
TUBA4A	P68366	Tubulin alpha-4A chain	24	0.68	0.0002
PMM2	O15305	Phosphomannomutase 2	20	0.68	0.0009
CNPY2	Q9Y2B0	Protein canopy homolog 2	24	0.68	0.0003
PTPRC	P08575	Receptor-type tyrosine-protein phosphatase C	23	0.68	0.0004
S100A9	P06702	Protein S100-A9	24	0.68	0.0003
LMAN1	P49257	Protein ERGIC-53	24	0.68	0.0003
EEF1G	P26641	Elongation factor 1-gamma	24	0.67	0.0004
STAT1	P42224	Signal transducer and activator of transcription 1-alpha/beta	23	0.66	0.0007
GBP1	P32455	Interferon-induced guanylate-binding protein 1	24	0.65	0.0005
GNB2L1	P63244	Guanine nucleotide-binding protein subunit beta-2-like 1	24	0.65	0.0006
PARP1	P09874	Poly [ADP-ribose] polymerase 1	24	0.64	0.0007
PFN1	P07737	Profilin-1	24	0.64	0.0008
HYOU1	Q9Y4L1	Hypoxia up-regulated protein 1 (GRP170)	24	0.63	0.0009
GANAB	Q14697	Neutral alpha-glucosidase AB	24	0.63	0.001
TNXB	P22105	Tenascin-X	23	-0.65	0.0008
CRTAC1	Q9NQ79	Cartilage acidic protein 1	22	-0.66	0.0009
HSPA1A	P0DMV8	Heat shock 70 kDa protein 1A/1B (HSP70-1)	24	-0.66	0.0005
SPTBN1	Q01082	Spectrin beta chain. non-erythrocytic 1	24	-0.67	0.0003
SNTB2	Q13425	Beta-2-syntrophin	24	-0.67	0.0004
LEMD2	Q8NC56	LEM domain-containing protein 2	21	-0.67	0.0008
LMNB2	Q03252	Lamin-B2	24	-0.68	0.0003
CKB	P12277	Creatine kinase B-type	20	-0.68	0.0009
GPX3	P22352	Glutathione peroxidase 3	23	-0.69	0.0002
CPQ	Q9Y646	Carboxypeptidase Q	18	-0.75	0.0004
SYNE3	Q6ZMZ3	Nesprin-3	23	-0.75	< 0.0001
SCARA5	Q6ZMJ2	Scavenger receptor class A member 5	15	-0.85	< 0.0001

Table 3: Correlation parameters between S100A8/S100A9 and the 50 protein intensities correlated to the histological score

Alarmins S100A8 and S100A9 were both correlated to the 50 other protein intensities obtained by MS/MS and correlated to the histological score. r = coefficient correlation (Pearson test). *, **, *** represent P-values < 0.05; 0.01 and 0.001, respectively. ns = not significant

	S100A8			**S100A9**	
	Pearson r	P value		Pearson r	P value
Protein S100-A9	0.9545	***		0.9545	***
Neutrophil defensin	0.9131	***		0.8637	***
Lymphocyte-specific protein 1	0.8527	***		0.8197	***
Coronin-1A	0.8417	***		0.8041	***
Plastin-2	0.837	***		0.8021	***
Cathepsin Z	0.8266	***		0.7937	***
Myeloid cell nuclear differentiation antigen	0.8118	***		0.7771	***
Tapasin	0.7384	***		0.6698	**
Profilin-1	0.7348	***		0.6748	***
Mesencephalic astrocyte-derived neurotrophic factor	0.7223	***		0.7417	***
Cathepsin S	0.7125	***		0.6177	**
Receptor-type tyrosine-protein phosphatase C	0.707	***		0.643	***
Rho GDP-dissociation inhibitor 2	0.6958	***		0.6217	**
Calreticulin	0.68	***		0.6088	**
Cytosol aminopeptidase	0.679	***		0.6264	**
Marginal zone B- and B1-cell-specific protein	0.667	**		0.7098	**
Elongation factor 1-gamma	0.6522	***		0.5827	**
Lamin-B1	0.6505	***		0.587	**
Echinoderm microtubule-associated protein-like 4	0.6346	**		0.5933	**
Phosphomannomutase 2	0.614	**		0.6091	**
Endoplasmic reticulum resident protein 29	0.5962	**		0.644	***
Peroxiredoxin-4	0.578	**		0.5787	**
Protein canopy homolog 2	0.5758	**		0.6744	***
Signal transducer and activator of transcription 1-alpha/beta	0.5704	**		0.5427	**
DnaJ homolog subfamily B member 11	0.5504	**		0.5635	**
Interferon-induced guanylate-binding protein 1	0.5373	**		0.566	**
Hypoxia up-regulated protein 1 (GRP170)	0.5357	**		0.5298	**
78 kDa glucose-regulated protein (GRP78) or BiP	0.5233	**		0.5043	*
Endoplasmin	0.5164	**		0.4804	*
Isocitrate dehydrogenase [NADP], mitochondrial	0.5118	*		0.4164	*
Protein disulfide-isomerase A4	0.5076	*		0.4499	*
Protein ERGIC-53	0.4971	*		0.4479	*
Tubulin alpha-4A chain	0.4941	*		0.4951	*
Neutral alpha-glucosidase AB	0.483	*		0.396	ns
Guanine nucleotide-binding protein subunit beta-2-like	0.4502	*		0.3353	ns
Signal recognition particle subunit SRP72	0.4444	*		0.4308	*
Thioredoxin domain-containing protein 5	0.4049	*		0.4182	*
Poly [ADP-ribose] polymerase 1	0.3561	ns		0.2772	ns
Cartilage acidic protein 1	-0.3355	ns		-0.3434	ns
Heat shock 70 kDa protein 1A/1B (HSP70-1)	-0.5366	**		-0.5838	**
LEM domain-containing protein 2	-0.6254	**		-0.5722	**
Nesprin-3	-0.6296	**		-0.6015	**
Tenascin-X	-0.6321	**		-0.5679	**
Spectrin beta chain, non-erythrocytic 1	-0.6884	***		-0.6734	***
Scavenger receptor class A member 5	-0.7069	**		-0.6619	**
Carboxypeptidase Q	-0.7156	***		-0.7019	**
Lamin-B2	-0.7414	***		-0.7293	***
Glutathione peroxidase 3	-0.7475	***		-0.7667	***
Beta-2-syntrophin	-0.7522	***		-0.8171	***
Creatine kinase B-type	-0.7555	***		-0.7136	***

Figures

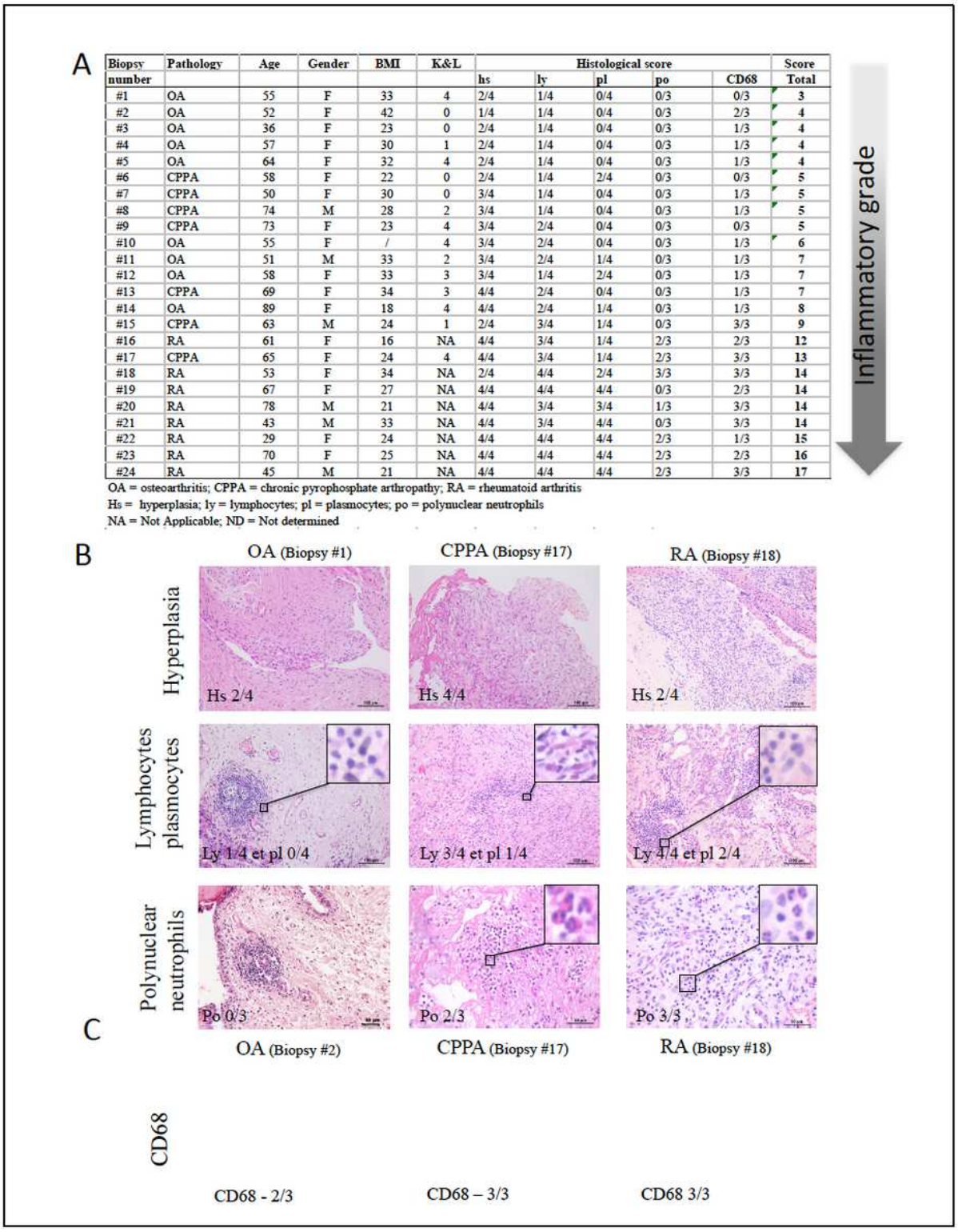

A

Biopsy number	Pathology	Age	Gender	BMI	K&L	Histological score					Score
						hs	ly	pl	po	CD68	Total
#1	OA	55	F	33	4	2/4	1/4	0/4	0/3	0/3	3
#2	OA	52	F	42	0	1/4	1/4	0/4	0/3	2/3	4
#3	OA	36	F	23	0	2/4	1/4	0/4	0/3	1/3	4
#4	OA	57	F	30	1	2/4	1/4	0/4	0/3	1/3	4
#5	OA	64	F	32	4	2/4	1/4	0/4	0/3	1/3	4
#6	CPPA	58	F	22	0	2/4	1/4	2/4	0/3	0/3	5
#7	CPPA	50	F	30	0	3/4	1/4	0/4	0/3	1/3	5
#8	CPPA	74	M	28	2	3/4	1/4	0/4	0/3	1/3	5
#9	CPPA	73	F	23	4	3/4	2/4	0/4	0/3	0/3	5
#10	OA	55	F	/	4	3/4	2/4	0/4	0/3	1/3	6
#11	OA	51	M	33	2	3/4	2/4	1/4	0/3	1/3	7
#12	OA	58	F	33	3	3/4	1/4	2/4	0/3	1/3	7
#13	CPPA	69	F	34	3	4/4	2/4	0/4	0/3	1/3	7
#14	OA	89	F	18	4	4/4	2/4	1/4	0/3	1/3	8
#15	CPPA	63	M	24	1	2/4	3/4	1/4	0/3	3/3	9
#16	RA	61	F	16	NA	4/4	3/4	1/4	2/3	2/3	12
#17	CPPA	65	F	24	4	4/4	3/4	1/4	2/3	3/3	13
#18	RA	53	F	34	NA	2/4	4/4	2/4	3/3	3/3	14
#19	RA	67	F	27	NA	4/4	4/4	4/4	0/3	2/3	14
#20	RA	78	M	21	NA	4/4	3/4	3/4	1/3	3/3	14
#21	RA	43	M	33	NA	4/4	3/4	4/4	0/3	3/3	14
#22	RA	29	F	24	NA	4/4	4/4	4/4	2/3	1/3	15
#23	RA	70	F	25	NA	4/4	4/4	4/4	2/3	2/3	16
#24	RA	45	M	21	NA	4/4	4/4	4/4	2/3	3/3	17

Inflammatory grade

OA = osteoarthritis; CPPA = chronic pyrophosphate arthropathy; RA = rheumatoid arthritis
Hs = hyperplasia; ly = lymphocytes; pl = plasmocytes; po = polynuclear neutrophils
NA = Not Applicable; ND = Not determined

Figure 1

Histological scoring of synovial biopsies A) Classification of OA, CPPA and RA synovial biopsies (n = 24) according to the histological score based on the following criteria: synovial hyperplasia (hs, 0 – 4), infiltration of lymphocytes (ly, 0 – 4), plasmocytes (pl, 0 – 4), polynuclear neutrophils (po, 0 – 3) and

macrophages (CD68, 0 – 3). B) Histological representation of hematoxylin eosin stained sections for synovial hyperplasia and infiltration of lymphocytes/plasmocytes and polynuclear neutrophils in one OA, CPPA or RA biopsy. C) Immunohistochemistry using anti-CD68 antibody showing macrophage infiltration in OA, CPPA and RA synovial biopsies.

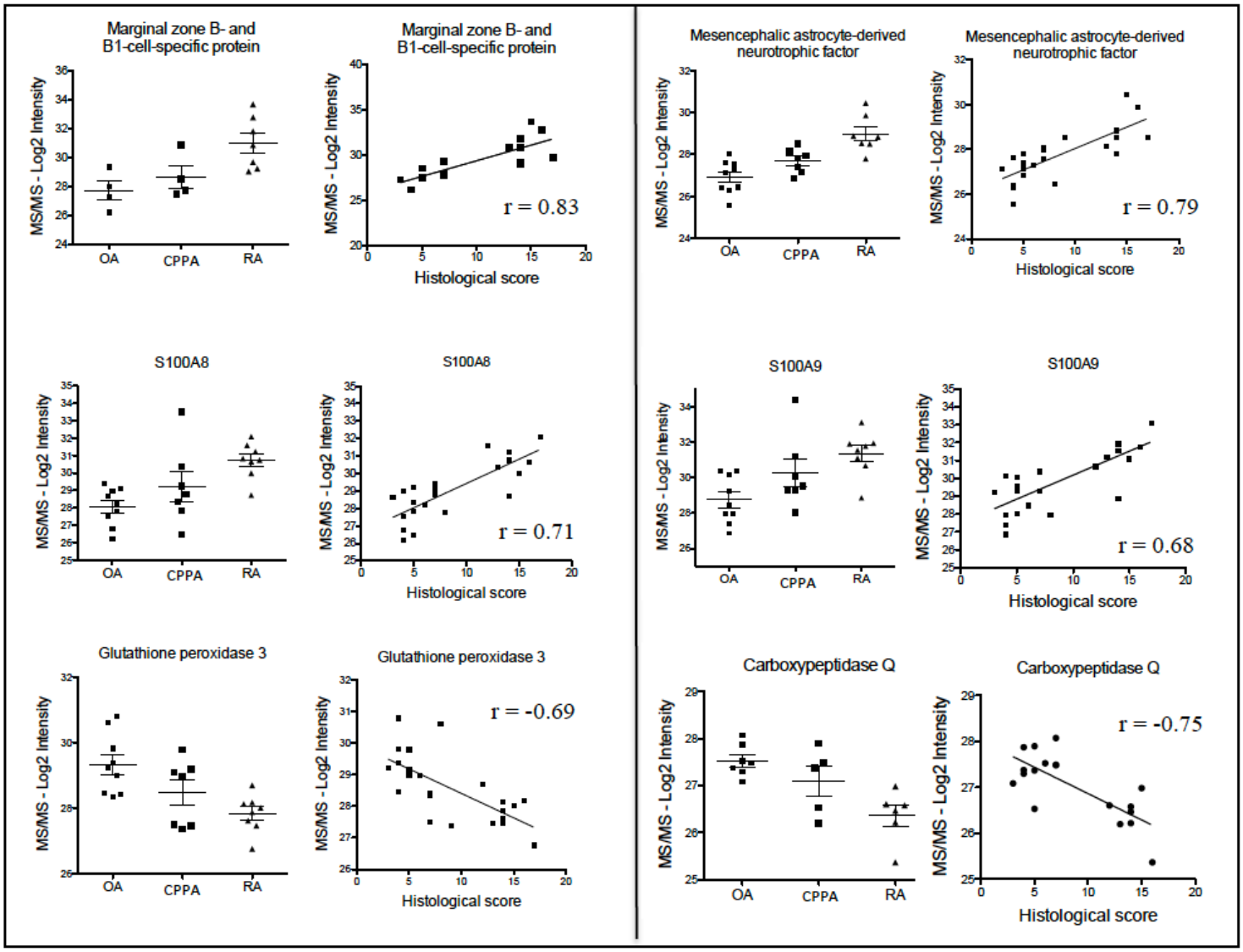

Figure 2

Distribution of protein intensities among the 3 groups (OA, CPPA and RA) and correlation with the histological score Illustration of some proteins from Table 2 for which log2 intensities obtained by MS/MS are represented among the three groups (OA, CPPA and RA) and statistically correlated to the histological score.

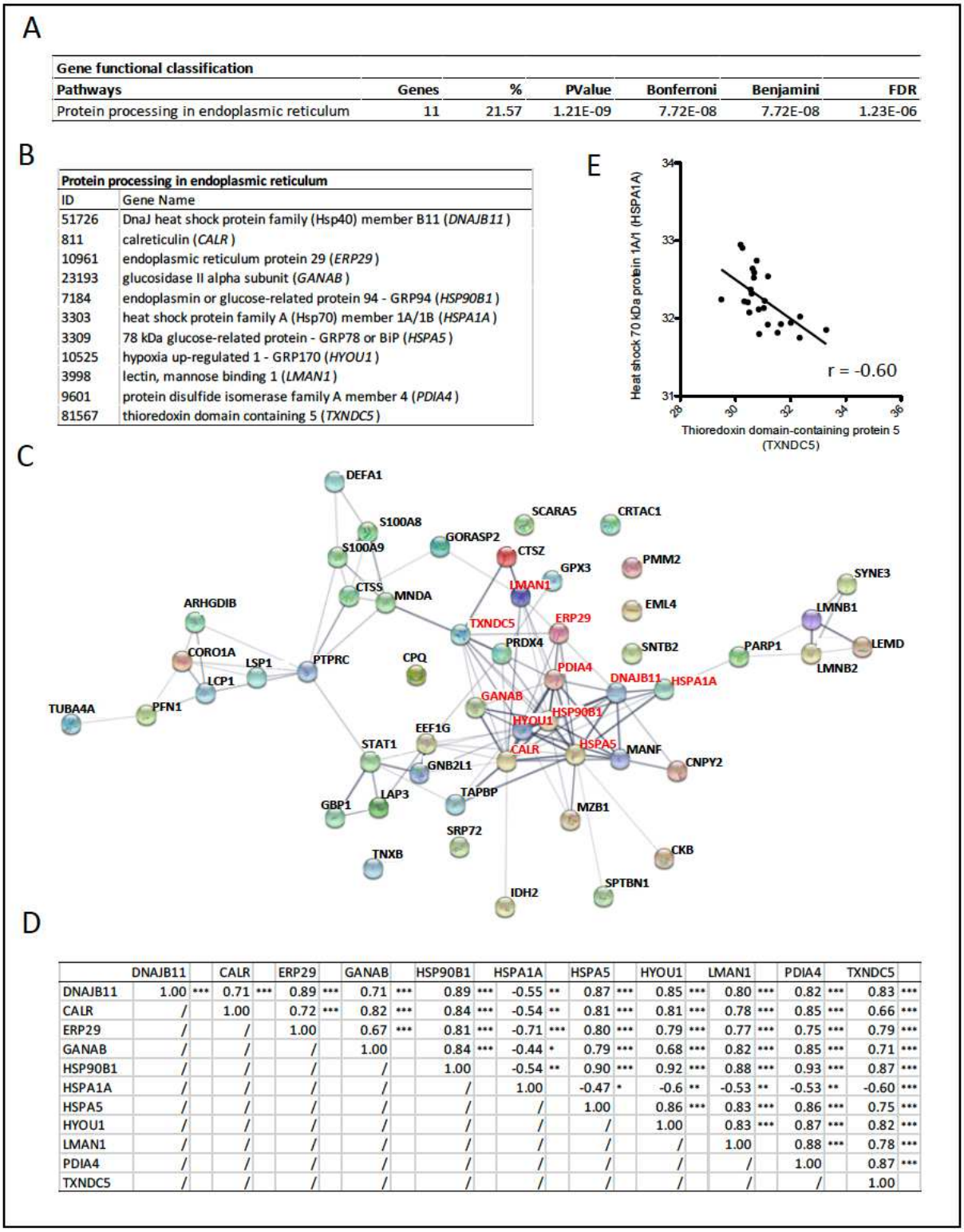

	DNAJB11		CALR		ERP29		GANAB		HSP90B1		HSPA1A		HSPA5		HYOU1		LMAN1		PDIA4		TXNDC5	
DNAJB11	1.00	***	0.71	***	0.89	***	0.71	***	0.89	***	-0.55	**	0.87	***	0.85	***	0.80	***	0.82	***	0.83	***
CALR	/		1.00		0.72	***	0.82	***	0.84	***	-0.54	**	0.81	***	0.81	***	0.78	***	0.85	***	0.66	***
ERP29	/		/		1.00		0.67	***	0.81	***	-0.71	***	0.80	***	0.79	***	0.77	***	0.75	***	0.79	***
GANAB	/		/		/		1.00		0.84	***	-0.44	*	0.79	***	0.68	***	0.82	***	0.85	***	0.71	***
HSP90B1	/		/		/		/		1.00		-0.54	**	0.90	***	0.92	***	0.88	***	0.93	***	0.87	***
HSPA1A	/		/		/		/		/		1.00		-0.47	*	-0.6	**	-0.53	**	-0.53	**	-0.60	***
HSPA5	/		/		/		/		/		/		1.00		0.86	***	0.83	***	0.86	***	0.75	***
HYOU1	/		/		/		/		/		/		/		1.00		0.83	***	0.87	***	0.82	***
LMAN1	/		/		/		/		/		/		/		/		1.00		0.88	***	0.78	***
PDIA4	/		/		/		/		/		/		/		/		/		1.00		0.87	***
TXNDC5	/		/		/		/		/		/		/		/		/		/		1.00	

Figure 3

ER stress proteins detected in the inflamed synovial membrane: A) DAVID analysis performed on the 51 biomarkers highlighted for their significant correlation to the histological score, for their functional classifications. The pathway entitled “protein processing in endoplasmic reticulum (ER)” was selected. B) Proteins involved in the ER pathway according to DAVID analysis. C) STRING protein-protein interaction among the 51 proteins highlighted in Table 2. Red writings indicate proteins involved in the ER network

according to DAVID analysis. D) Correlation parameters between the 11 proteins involved in the ER according to DAVID. E) Negative correlation between HSPA1A and TXNDC5 protein levels.

Supplementary Files

This is a list of supplementary files associated with this preprint. Click to download.

- Additionalfile1.pdf